University of Tartu
Institute of Computer Science
Data Science Curriculum

Ares Hubel

Exploring Entropy and Signal Diversity in Neural Networks Using the AdEx Model

Master's Thesis (15 ECTS)

Supervisor(s):
Karl Kristjan Kaup, Master's Degree - PhD student in University of Tartu

Tartu 2025

Exploring Entropy and Signal Diversity in Neural Networks Using the AdEx Model

Abstract:

The intricate activity of neural systems presents a significant frontier in scientific understanding. This master's thesis delves into this complexity by computationally investigating entropy and signal diversity, which are key metrics for characterizing information processing in the brain. Employing Adaptive Exponential Integrate-and-Fire (AdEx) neural network models, the research systematically explores how fundamental neuronal and network parameters, including synaptic delay, weight, and connectivity patterns, influence the dynamic behavior of these networks. This investigation also aims to deepen the understanding of the AdEx model's operational characteristics under varied conditions. The study quantifies these influences through Shannon Entropy (SE) of spike train activity and Lempel-Ziv Complexity (LZC) derived from spike train patterns. The overarching goals are to clarify the mechanisms by which specific parameters govern signal richness, to further elucidate the workings of the AdEx model, and to assess the implications of the findings for theories like the Entropic Brain Hypothesis.

Keywords: AdEx model, Neural networks, Computational neuroscience, Neural entrophy

CERCS: P170 Computer science, numerical analysis, systems, control

Visual Abstract:

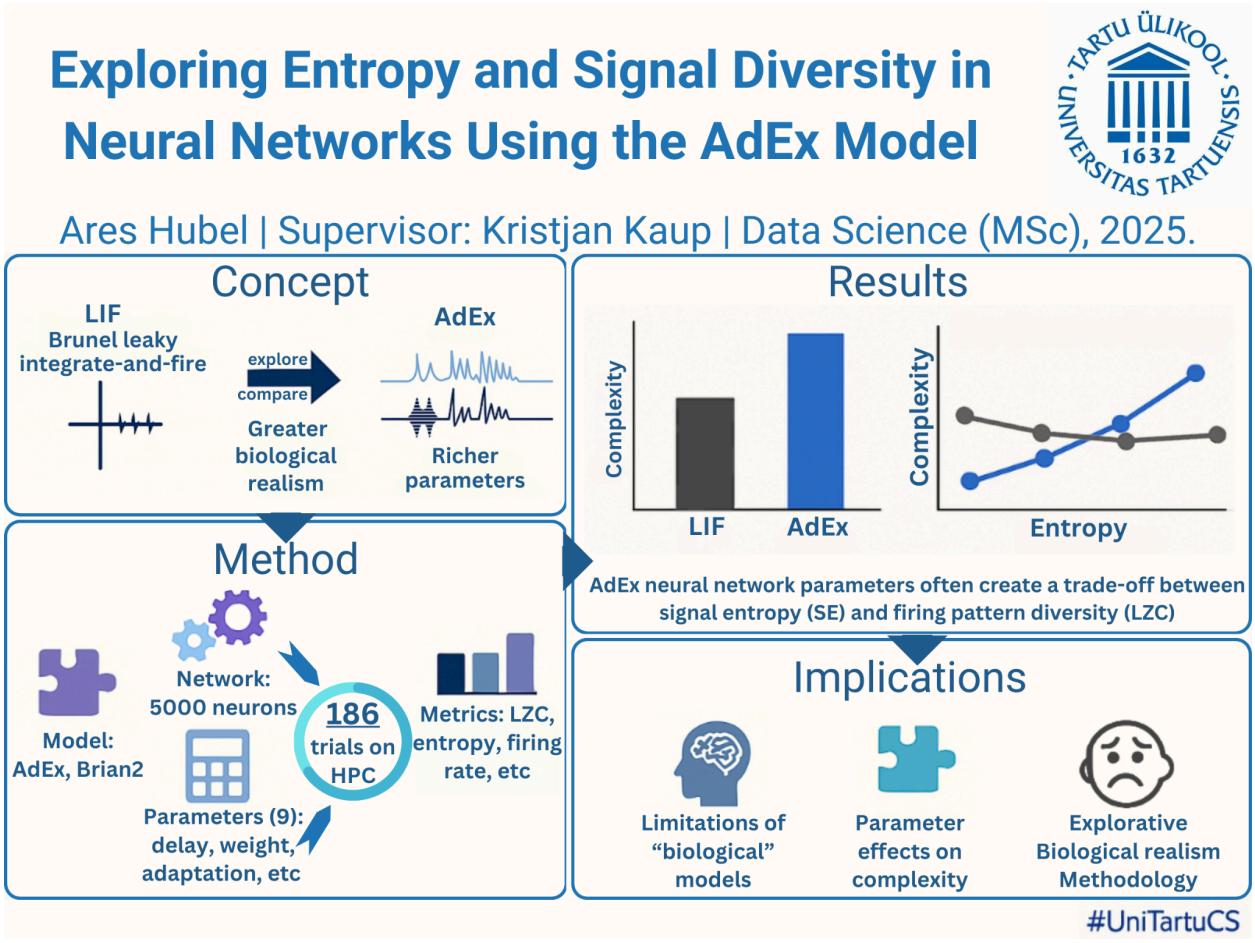

Entroopia ja signaali mitmekesisuse uurimine AdEx närvivõrkudes

Lühikokkuvõte:

Närvisüsteemide keerukas aktiivsus kujutab endast olulist teadusliku mõistmise piiriala. Käesolev magistritöö süveneb sellesse keerukusse, uurides arvutuslikult entroopiat ja signaali mitmekesisust, mis on aju infotöötluse iseloomustamisel keskse tähtsusega näitajad. Kasutades adaptiivseid eksponentsiaalseid integreeri-ja-käivita (AdEx) närvivõrgu mudeleid, uurib töö süstemaatiliselt, kuidas fundamentaalsed neuronaalsed ja võrgu parameetrid, sealhulgas sünaptiline viivitus, kaal ja ühenduvusmustrid, mõjutavad nende võrkude dünaamilist käitumist. Ühtlasi on uurimuse eesmärgiks süvendada arusaamist AdEx mudeli toimimise iseärasustest erinevates tingimustes. Uuring kvantifitseerib neid mõjusid aktsioonipotentsiaalide jadade Shannoni entroopia (SE) ja aktsioonipotensiaalide mustritest tuletatud Lempel-Zivi komplekssuse (LZC) kaudu. Üldised eesmärgid on selgitada mehhanisme, mille abil spetsiifilised parameetrid juhivad signaali mitmekesisust, täiendavalt valgustada AdEx mudeli toimimist ning hinnata leidude tähendust teooriate, nagu entroopilise aju hüpotees, jaoks.

Võtmesõnad: AdEx mudel, Närvivõrgud, Arvutuslik neuroteadus, Neuraalne entroopia

CERCS: P170 Arvutiteadus, arvutusmeetodid, süsteemid, juhtimine (automaatjuhtimisteooria)

Visuaalne kokkuvõte:

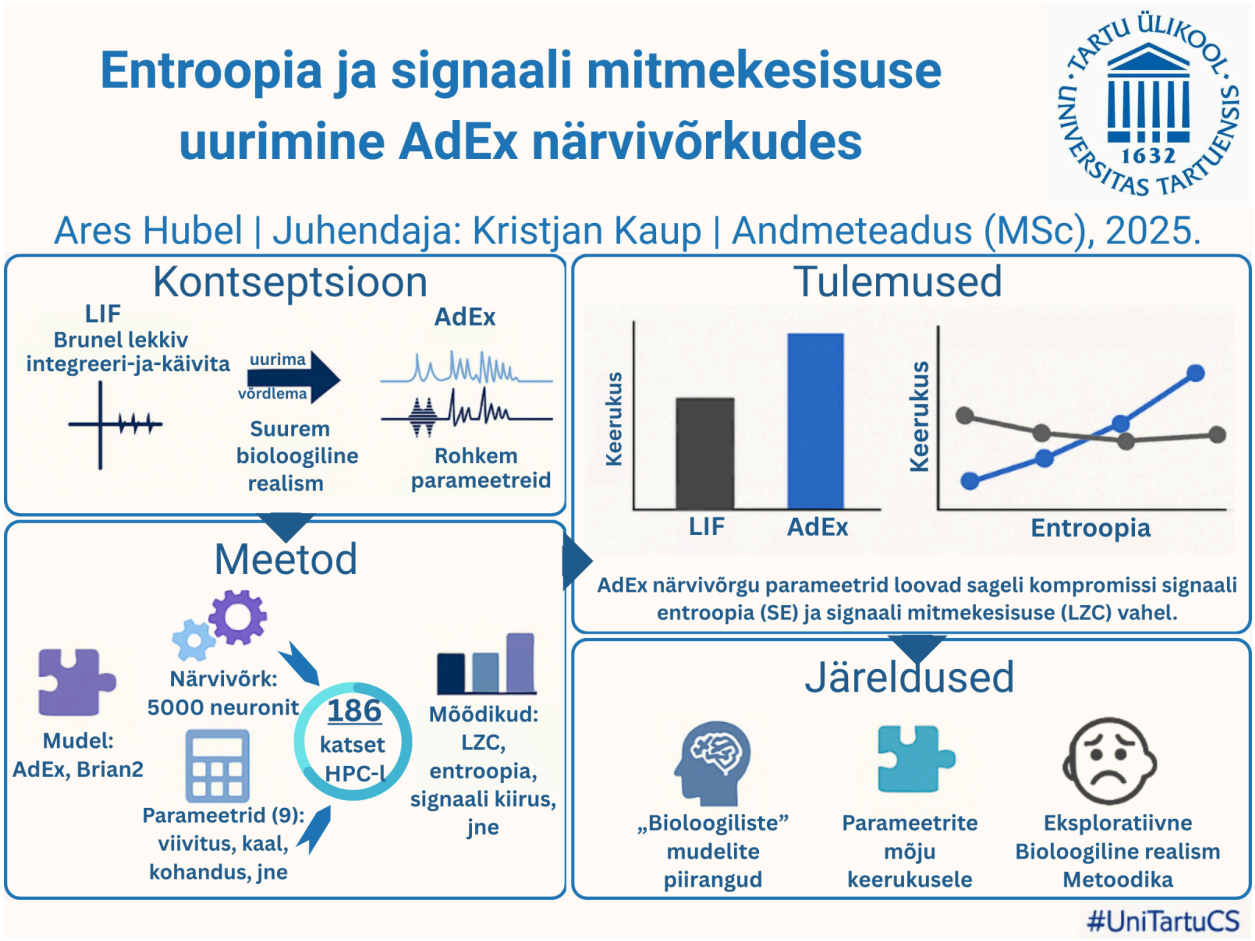

Table of Contents

1. Introduction

The human brain is an incredibly complex system. It produces a vast range of neural activity that is the basis for how we think, perceive the world, and experience consciousness. A major goal in neuroscience is to understand the rules that govern these neural activities. In recent years, ideas from information theory, like entropy and complexity, have given us useful mathematical tools. These tools help us understand the richness, predictability, and information processing capabilities of neural systems..

Neural entropy is a measure of how varied and unpredictable brain signals are. It's increasingly seen as an important part of healthy brain function and a possible sign of conscious states (Carhart-Harris, 2018; Tononi et al., 1994). This idea is key to the Entropic Brain Hypothesis (EBH).. The EBH suggests that there is a direct link between how much entropy is in neural activity and how rich our conscious experience is (Carhart-Harris et al., 2014; Carhart-Harris, 2018). According to the EBH, different states of consciousness can be placed on a scale of neural entropy. In a normal waking state, our consciousness shows a balanced level of entropy. Significant changes from this balance, i.e too little entropy (as in a coma or deep sleep) or too much (as in acute psychosis or potentially with psychedelic drugs), are connected to altered or diminished states of awareness. (Carhart-Harris, 2018). Psychedelic substances like psilocybin and LSD are interesting in this context because they seem to increase neural entropy. This increase is thought to be related to the major changes in consciousness they cause and their potential benefits as treatments (Carhart-Harris et al., 2014; Ruffini et al., 2023). Neuroimaging studies, particularly EEG, show that measures like Lempel-Ziv Complexity (LZC), often seen as a sign of entropy, go up when psychedelic drugs are used (Schartner et al., 2017; Aamodt et al., 2021). While these studies typically derive LZC from continuous field potentials, the concept of quantifying signal diversity is broadly relevant. However, results from other methods like functional magnetic resonance imaging (fMRI) can differ more (McCulloch et al., 2023; Singleton et al., 2022), which shows we still need more research and stronger theories.

Beyond consciousness and psychedelic states, neural entropy and signal diversity (which describes the complexity and variety of brain activity) are important for understanding general brain function and problems. Unusual levels of entropy have been found in several psychiatric and neurological conditions, like schizophrenia and depression, suggesting that information processing might be disrupted (Sabeti et al., 2009; Kalev et al., 2015; Farnes et al., 2020). Neuroimaging provides valuable data from living brains, but the brain's complexity makes it difficult to identify the precise neural mechanisms behind changes in entropy and complexity (Fagerholm et al., 2023).

Computational modeling gives us another powerful way to study these mechanisms in a controlled computer environment. Simulating neural networks allows researchers to

systematically study how specific cellular and network details influence overall activity, including entropy and complexity measures.

This thesis uses the Adaptive Exponential Integrate-and-Fire (AdEx) neuron model. The AdEx model is a good choice for this research because it can create a wide variety of realistic neuron firing patterns due to a feature called an adaptation current (Naud et al., 2008; Brette & Gerstner, 2005). Because it can create varied signals, it's good for studying how different factors change measures of information, like spike train entropy (Shannon Entropy - SE) and Lempel-Ziv Complexity (LZC). SE is calculated from the temporal distribution of network spike counts, while our LZC measure quantifies the diversity of instantaneous population firing patterns derived directly from neuronal spike activity. The LFP, which represents the combined, filtered activity of nearby neurons as if measured by a virtual electrode, helps connect single-neuron activity to the larger signals we see in experiments.

Importantly, we set up the AdEx model's baseline to match an earlier project that used a simpler Leaky Integrate-and-Fire (LIF) model (Wierzchula et al., 2024). The baseline configuration can be found in Methods section Table 1. Matching certain output features in this way allows us to more directly compare how entropy and signal diversity act in models with different levels of complexity. While the AdEx model is capable of significant biological realism (Naud et al., 2008), its specific configuration here prioritizes this comparability alongside its inherent ability to generate diverse firing patterns necessary for studying entropy and complexity.

This research aims to use the AdEx model to explore the connections between basic neural and network parameters, the resulting neural activity, and key measures of complexity and entropy. These measures are relevant to the Entropic Brain Hypothesis and understanding how brain-like systems process information. Specifically, this study will simulate a network of AdEx neurons and systematically change parameters such as:

- Synaptic delay (D)
- Synaptic weight (J)
- Spike threshold (V_T)
- Subthreshold adaptation (a)
- Connection probability (epsilon)
- Relative inhibitory synaptic strength (g)
- The balance between excitatory and inhibitory neurons (gamma)
- Noise intensity (sigma)
- Neuronal refractory period (tau_rp)

The effects of these changes will be measured through Shannon Entropy (SE) of spike trains, and Lempel-Ziv Complexity (LZC) of simulated LFPs. We will also look at characteristics of the

LFP (mean and standard deviation) and average firing rates.

The main objectives of this thesis are:

1. To investigate how varying key AdEx neuron and network parameters (D, J, V_T, a, epsilon, g, gamma, sigma, tau_rp) affects Shannon Entropy (SE) of spike trains and Lempel-Ziv Complexity (LZC) of simulated Local Field Potentials. This aims to find which parameters most strongly influence these measures of entropy and complexity.
2. To analyze the relationship between SE and LZC as these AdEx parameters are changed.
3. To compare the AdEx model to a LIF model used in an earlier project (Wierzchula et al., 2024).
4. To critically discuss the findings in terms of how neural and network parameters shape signal diversity in AdEx neural networks, and to explore their potential relevance to the Entropic Brain Hypothesis, while maintaining a cautious and critical perspective on direct biological claims.

By addressing these goals, this research aims to better explain how specific neural parameters influence the complex activity and information-handling features of brain-like networks. The results aim to contribute to computational neuroscience, offering insights relevant to information processing in neural systems and theoretical ideas like the EBH.

Generative AI tools (Grok;Gemini in Google Colab) have been used for scripting and editing purposes in context of this work.

2. Methods

This section describes the computational model, how the simulations were set up and run, the methods for data analysis, and how we defined the measures used to study the effects of Adaptive Exponential (AdEx) integrate-and-fire neuron and network parameters on neural entropy and complexity.

2.1 Computational Model and Network Architecture

We used the Adaptive Exponential (AdEx) integrate-and-fire neuron model for our simulations, implemented with the Brian 2 simulator (Stimberg et al., 2019). The AdEx model is helpful because its adaptation mechanism lets it copy many realistic neuron firing patterns found in the brain (Naud et al., 2008; Brette & Gerstner, 2005). The behavior of each AdEx neuron is described by two equations that show how its membrane potential (Vm) and an adaptation current (w) change over time:

$$C\frac{dV_m}{dt} = -g_L(V_m - E_L) + g_L\Delta_T \exp\left(\frac{V_m - V_T}{\Delta_T}\right) - w + I_{syn} + I_{noise}$$

$$\tau_w \frac{dw}{dt} = a(V_m - E_L) - w$$

Here's what the symbols mean:

- C: Membrane capacitance
- V_m: Membrane potential
- V_r: Reset potential
- g_L: Leak conductance
- E_L: Leak reversal potential
- Δ_T: Slope factor
- V_T (V_T): Spike threshold
- w: Adaptation current
- I_{syn}: Synaptic current
- I_{noise}: Noise current
- τ_w (tau_w): Adaptation time constant
- τ_{rp} (tau_rp): Refractory period
- a: Subthreshold adaptation coupling
- b: Spike-triggered adaptation increment
- dt: Time step for Euler method

A neuron fires a spike when its membrane potential V_m crosses a certain level called V_{cut} (defined as $V_T+5\Delta_T$). After a spike, V_m is reset to a value V_r, the adaptation current w is increased by an amount b (spike-triggered adaptation), and the neuron cannot fire again for a brief period called the refractory period (tau_rp). We used the Euler method with a time step (dt) of 0.1 ms to solve these equations in the simulations.

The simulated network contained N=5000 neurons. We chose this network size because it's big enough to show complex network actions (Brunel, 2000) but small enough to handle the many simulations required. Of these neurons, 80% were excitatory (N_E=4000), meaning they tend to make other neurons fire, and 20% were inhibitory (N_I=1000; gamma=0.2), meaning they tend to prevent other neurons from firing. This 80/20 ratio is a common approximation for parts of the brain like the cortex (Brunel, 2000).

Setting Baseline Parameters for Comparison: A crucial aspect of this study is that the baseline parameters for the AdEx neurons were chosen not primarily for direct biological realism of a specific cell type (cf. Gerstner et al., 2014; Naud et al., 2008), but to ensure that the network's output characteristics could be meaningfully compared to results from a previous project using a

simpler Leaky Integrate-and-Fire (LIF) model (Wierzchula et al., 2024). This previous LIF project used specific parameters, and the AdEx model was configured to produce broadly comparable activity levels and dynamics. The parameters for the excitatory (RS-like) and inhibitory (FS-like) AdEx neurons used as a baseline in this study are detailed in Table 1 below. When a specific parameter was varied in our tests, it was typically applied to both excitatory and inhibitory neuron populations, unless the parameter itself defined the populations (like gamma).

The final python script and HPC setup configurations for the parameter testing can be found in the Appendises (Appendix 1: adex_simulation.py, Appendix 2: submit_experiements.sh, Appendix 3: run_adex.sh, Appendix 4: HPC setup).

Table 1: Baseline AdEx Neuron Parameters

Parameter	**Symbol**	**Excitatory (RS-like) Value**	**Inhibitory (FS-like) Value**	**Unit**
Membrane Capacitance	C	150	100	pF
Leak Conductance	g_L	10	10	nS
Leak Reversal Potential	E_L	-65	-65	mV
Spike Threshold	V_T	-50	-42	mV
Slope Factor	Delta_T	2	2	mV
Subthreshold Adaptation	a	2	0	nS
Adaptation Time Constant	tau_w	500	15	ms
Spike-triggered Adaptation	b	0.01	0	nA
Reset Potential	V_r	-60	-65	mV
Refractory Period	tau_rp	2	1	ms

Neurons in the network were connected randomly. The baseline probability of connection between any two neurons was 'epsilon'. Excitatory connections had a strength (weight) 'J', and inhibitory connections had a strength of '−g*J' (where 'g' is the relative inhibitory strength). All connections had a transmission delay 'D'. The network also received random excitatory input from an external source, modeled as Poisson spike trains, at a rate (nuext) designed to keep the network in a balanced state where activity is irregular, similar to what is observed in the cortex (Vogels & Abbott, 2005).

2.2 Simulation Protocol and Parameter Variation

Each simulation was run for 1 second of model time. For the main experiments, we varied one parameter at a time, keeping others at their baseline values (as in Table 1, with J=0.04 mV). We ran three independent trials for each parameter value to check for consistency. The parameters we varied, and the range of values tested, are listed below:

- **Synaptic Delay (D):** 0.3, 0.6, 0.9, 1.2, 1.5 (baseline), 1.8, 2.1, 2.4 ms.
- **Excitatory Synaptic Weight (J):** 0.02, 0.04 (baseline), 0.06, 0.08, 0.10, 0.12, 0.14, 0.16, 0.18 mV.
- **Relative Inhibitory Strength (g):** 1.4, 2.8, 4.2, 5.6 (close to baseline of 5 in LIF project), 7.0, 8.4, 9.8, 11.2, 12.6.
- **E/I Neuron Ratio (gamma - proportion of inhibitory neurons):** 0.05, 0.10, 0.15, 0.20 (baseline), 0.25, 0.30, 0.35, 0.40, 0.45.
- **Connection Probability (epsilon):** 0.02, 0.04, 0.06, 0.08, 0.10 (baseline), 0.12, 0.14, 0.16, 0.18.
- **Refractory Period (tau_rp):** 0.4, 0.8, 1.2, 1.6, 2.0 (baseline for excitatory), 2.4, 2.8, 3.2, 3.6 ms.
- **Subthreshold Adaptation (a):** 0.0, 2.0 (baseline for excitatory), 4.0 nS.
- **Noise Intensity (sigma - external noise current amplitude):** 0.0, 0.1 (baseline), 0.2 nA.
- **Spike Threshold (V_T):** -55.0, -50.0 (baseline for excitatory), -45.0 mV.

2.3 Data Generation and Metrics

From each simulation, we collected data to calculate several measures:

- **Spike Data & Mean Firing Rate (MFR):** We recorded the timing of every spike from every neuron using Brian 2's SpikeMonitor. The Mean Firing Rate (MFR) for the network was calculated as the total number of spikes divided by the number of neurons and the simulation duration (1 second), reported in Hertz (Hz).
- **Local Field Potential (LFP):** We simulated the LFP using a kernel-based method (Telenczuk et al., 2020; Mazzoni et al., 2008). This method calculates the LFP by adding up the effects of spikes from nearby neurons. Each spike's effect is adjusted over time and gets weaker the farther away it is. We used specific amplitudes for excitatory (amp_e = 0.48) and inhibitory (amp_i = 3) contributions, and Gaussian kernels with different widths for each (sig_e = 3.15, sig_i = 2.1). The LFP was calculated as a time-resolved signal, and from this, we found the LFP mean amplitude and LFP standard deviation (a measure of LFP signal fluctuation), both reported in microvolts (μV).
- **Spike Train Entropy (SE - Shannon Entropy):** To quantify the predictability or randomness of the network's spiking activity, we calculated Shannon Entropy. This was

done by dividing the 1-second simulation into bins of 0.2 seconds (5 bins total). We counted the total number of spikes across the entire network within each bin. This gave us a distribution of spike counts, and we calculated the Shannon entropy of this distribution. A higher SE means the pattern of total network activity across these large time bins is less predictable. This calculation is detailed in the *compute_se* function in the *adex_simulation.py* script (Appendix 1). The results are reported in bits.

- **Lempel-Ziv Complexity (LZC):** LZC measures the diversity of patterns in a sequence (Lempel & Ziv, 1976; Zhang et al., 2001). For each small time step (0.1 ms) of the simulation, we created a binary pattern representing which neurons in the network fired ('1') and which did not ('0'). The LZC algorithm was then applied to this sequence of instantaneous population firing patterns, and the results were averaged across time. This measures the diversity of different ways the whole population of neurons can fire together. A higher LZC indicates a richer repertoire of these population firing patterns.

2.4 Initial Network Setup and Baseline Characteristics

Before running the main parameter variations, we performed initial tests to establish a stable AdEx network that produced activity patterns broadly comparable to those from the previous LIF model study. This involved confirming the network size (N=5000), the baseline excitatory synaptic strength (J=0.04mV), and the bin size for SE calculation (0.2s). The baseline configuration (parameters from Table 1, J=0.04mV, gamma=0.2, epsilon=0.1, D=1.5ms, g=5, etc.) produced the following approximate average characteristics:

- Mean Firing Rate: ~7.18 Hz (std = 0.0061, ~0.09% variation) This baseline firing rate falls within ranges considered typical for spontaneous cortical activity (e.g., Buzsáki & Mizuseki, 2014; Zerlaut et al., 2018).
- Spike Train Entropy (SE): ~1.54 bits (std = 0.0056, ~0.36% variation, aligned with LIF's 1.53–1.60 bits)
- LFP Mean: ~174.94 μV
- LFP Standard Deviation: ~2.86 mV (or 2866 μV, std = 4.94 μV, ~0.17% variation)
- LZC: J=0.04mV (baseline for J), (~1.59, std = 0.0291, ~1.8% variation). (The AdEx model's adaptation mechanisms can influence firing pattern regularity (Ladenbauer et al., 2013; Touboul & Brette, 2008), affecting LZC.)

These values for MFR and LFP provided a basic operational state for the model, from which the effects of parameter variations on SE and LZC could be investigated.

2.5 Computational Resources and Output Validation

Simulations were performed using the University of Tartu's Rocket High-Performance

Computing (HPC) cluster. Each individual simulation (one parameter value, one trial) took approximately 0.5 to 2.5 hours on an HPC node. While this seems like a long duration per trial, we have to take into consideration AdEx model higher computational needs and possibly optimization issues with the scripts. Although moderate effort was allocated to optimizing the scripts, it is hard to verify how successful it was. Given 62 unique parameter conditions and 3 trials each, a total of 186 primary simulations were run, plus initial tuning runs and error correction runs. We carefully checked the output to make sure the data was accurate. This included testing if initial trials gave repeatable results (like a firing rate standard deviation of about 0.09% for the baseline), automatically recording and fixing errors (such as NaN values by limiting state variables), re-running failed trials, and using scripts to check that output CSV files were complete and had reasonable metric values (for example, a firing rate standard deviation less than 0.5 Hz). This ensured a reliable dataset for the analyses presented in this thesis.

3. Results

This section presents the findings of the simulations. First, we briefly describe the general activity characteristics of the baseline AdEx network model that was configured for comparability with an earlier LIF model. However, we mainly focus on how changing different neuron and network parameters step-by-step impacts two key measures: Spike Train Entropy (SE) and Lempel-Ziv Complexity (LZC).

3.1 Baseline Model Characteristics

The AdEx network, when set up with its baseline parameters (see Table 1 in Methods, e.g., J=0.04mV, gamma=0.2) chosen to allow comparison with a previous LIF model study, showed a certain level of activity. The average firing rate across the network was approximately 7.17 Hz. The simulated Local Field Potential (LFP) had an average amplitude of about 175.31 μV and a standard deviation (fluctuation) of about 2866.61 μV. These values simply characterize the operational state of our specific model setup before we started changing individual parameters to observe their effects on SE and LZC.

3.2 Parameter Effects on Spike Train Entropy (SE) and Lempel-Ziv Complexity (LZC)

We systematically varied nine key AdEx model parameters and observed their impact on SE (a measure of the unpredictability of network spike counts over time) and LZC (a measure of the diversity of instantaneous population firing patterns.

Figure 1 provides an overview of how SE and LZC (y-axes) change as different parameters (x-axes) are varied.

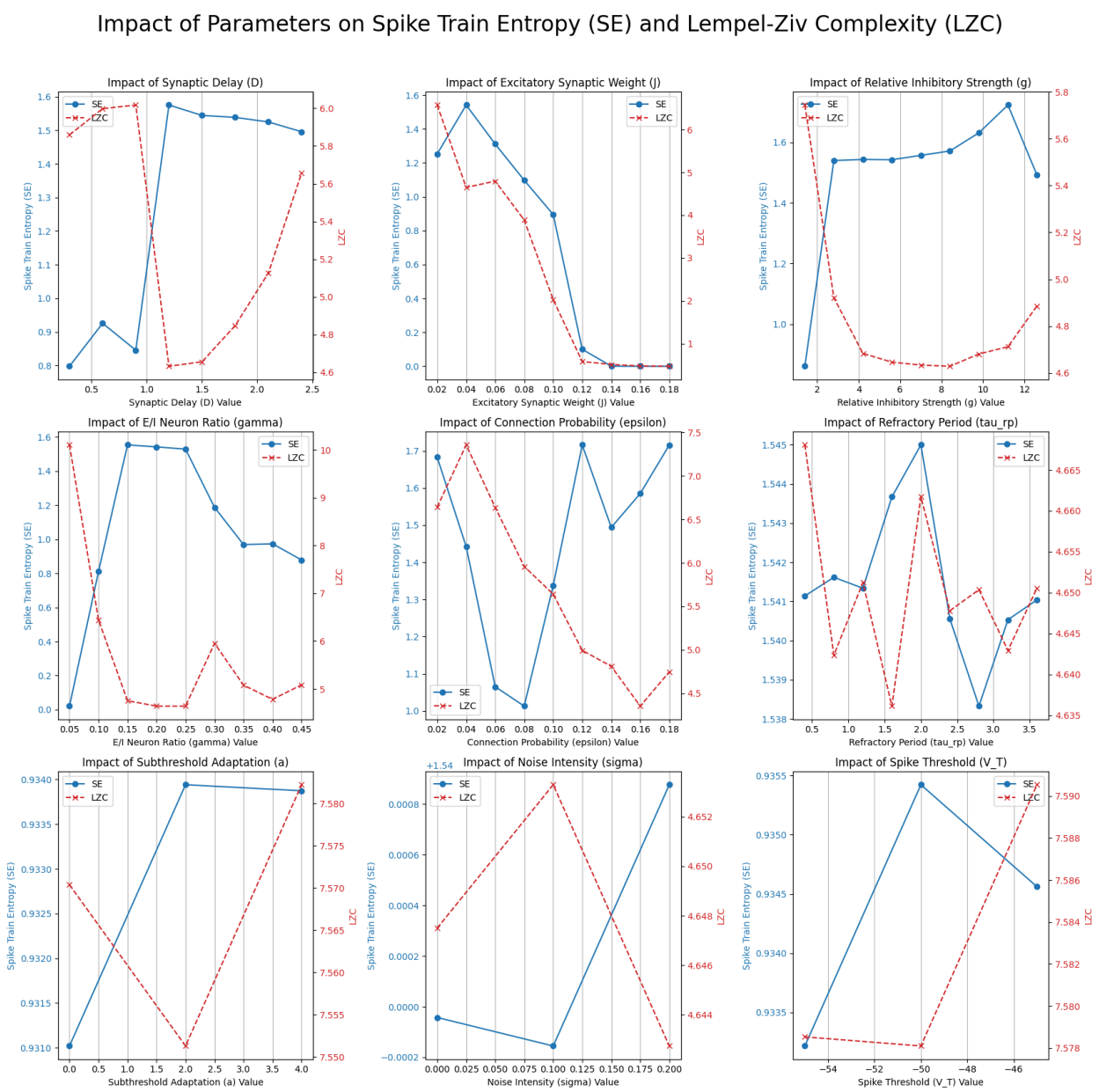

Figure 1. Impact of AdEx Model Parameters on Spike Train Entropy (SE) and Lempel-Ziv Complexity (LZC). Each subplot shows how SE (solid line, primary y-axis) and LZC (dashed line, secondary y-axis) respond to changes in a single AdEx model parameter (indicated on the x-axis and in the subplot title). Values are mean results from the simulations (mean of 3 trials).

Summary of How Parameters Affect SE and LZC:

- **Synaptic Delay (D):** SE peaked at 1.2 ms; lower at shorter/longer delays. LZC generally increased from 0.3 to 0.9 ms, then decreased.
- **Excitatory Synaptic Weight (J):** SE was highest at baseline J (0.04 mV) and decreased with higher J. LZC was highest at the lowest J (0.02 mV) and decreased with increasing

J.

- **Relative Inhibitory Strength (g):** SE generally increased with 'g', peaking at 11.2. LZC showed the opposite trend, decreasing as 'g' increased.
- **E/I Neuron Ratio (gamma):** SE was very low at low gamma (0.05), peaked at 0.15, then decreased. LZC peaked dramatically at the lowest gamma and was lower for higher gamma.
- **Connection Probability (epsilon):** SE was generally high across many epsilon values. LZC tended to be higher at lower epsilon and decreased as epsilon increased.
- **Refractory Period (tau_rp):** Minimal effect on SE and LZC; mean firing rates ~7.17-7.20 Hz.

For the **spike threshold (V_T)**, **subthreshold adaptation (a)**, and **noise intensity (sigma)**, only three distinct values were tested for each. This limited number of data points prevents any statistically meaningful conclusions about their broader impact or correlation between SE and LZC.

3.3 Relationship Between SE and LZC:

To understand if SE and LZC tend to increase or decrease together, we looked at their correlation when each parameter was varied. Table 2 shows these Pearson correlations. Note that for V_T, 'a', and sigma, only 3 data points were available for the correlation, making these specific correlations statistically less reliable.

Table 2: Pearson Correlation between SE and LZC.

Parameter	Pearson *r*	*p*-value	df	N_points
D	-0.86	**.006**	6	8
J	0.92	**< .001**	7	9
V_T	0.10	.939	1	3
a	-0.15	.902	1	3
epsilon	-0.42	.263	7	9
g	-0.94	**< .001**	7	9
gamma	-0.87	**.002**	7	9
sigma	-0.89	.306	1	3
tau_rp	0.07	.852	7	9

(Note: Correlations for V_T, a, sigma are based on N=3 points (df=1) and are statistically unreliable)

- **Significant Negative Correlations (SE vs. LZC):**
    - Variations in synaptic delay (D), relative inhibitory strength (g), and the E/I neuron ratio (gamma) all showed strong and statistically significant negative correlations. This means that when we changed these parameters, situations causing higher SE often went along with lower LZC, and the other way around. For example, increasing 'g' tended to increase SE but decrease LZC.
- **Significant Positive Correlation (SE vs. LZC):**
    - Only changes in excitatory synaptic weight (J) showed a strong, significant positive correlation. This suggests that as J was varied, SE and LZC tended to change in the same direction.
- **Weak or Non-Significant Correlations:**
    - For other parameters such as spike threshold (V_T), subthreshold adaptation (a), and noise intensity (sigma), the correlation coefficients are reported in Table 2 but are statistically unreliable due to the very limited number of data points (N=3), and thus no conclusions are drawn from them regarding the relationship between SE and LZC."

3.4 Important Network States

This part of the results shows specific settings for the model that created interesting network activity. We look mainly at states where excitation and inhibition (E/I) were balanced, and also states where both SE and LZC values were high at the same time.

Balanced E/I States (gamma = 0.15-0.25):
When the amount of inhibitory nerve cells (gamma) was between 0.15 and 0.25, the networks usually had average firing rates of about 6.9-7.4 Hz. These rates are similar to what is expected in the brain (e.g., Buzsáki & Mizuseki, 2014; Zerlaut et al., 2018). In these balanced states, the Spike Train Entropy (SE) was always high, around 1.53-1.55 bits (for gamma = 0.25 and gamma = 0.15 respectively). But, the Lempel-Ziv Complexity (LZC) was quite low, around 0.38-0.39 (for gamma = 0.20/0.25 and gamma = 0.15 respectively). This means that when E/I was balanced, the overall network activity was hard to predict over time (high SE), but there was less variety in how all the nerve cells fired together at any moment (low LZC).

States with High SE and LZC at the Same Time:
We also found model settings where both SE and LZC were above their typical (median) values from all tests, and the networks had realistic average firing rates (e.g., 1-15 Hz). One clear example was when the connection probability (epsilon) was low at 0.02. This setting gave an SE of about 1.683 bits, an LZC of about 0.540, and an average firing rate of about 5.07 Hz.

Other model settings that resulted in high SE and also medium or higher (above median) LZC were:

- epsilon = 0.12 (SE ≈ 1.716, LZC ≈ 0.406)
- gamma = 0.10 (SE ≈ 1.541, LZC ≈ 0.525)
- D = 0.9 ms (SE ≈ 0.845, LZC ≈ 0.490) - here SE is not very high, but LZC is.

These results show that different parameters have varied and sometimes opposing effects on SE and LZC, and that achieving states where both measures are high is possible but depends on specific parameter configurations.

3.5 Comparison of SE and LZC Trends with a Leaky Integrate-and-Fire (LIF) Model

To better understand the impact of the AdEx model's adaptive mechanisms, it is useful to compare its Shannon Entropy (SE) and Lempel-Ziv Complexity (LZC) responses to parameter variations with those from a simpler, non-adaptive Leaky Integrate-and-Fire (LIF) model. The following comparison (Figure 2) assumes a similar baseline configuration for both models, allowing us to highlight differences potentially from neuronal adaptation. The LIF model results are drawn from LIF project output (Wierzchula et al., 2024) (Appendix 5: LIF output).

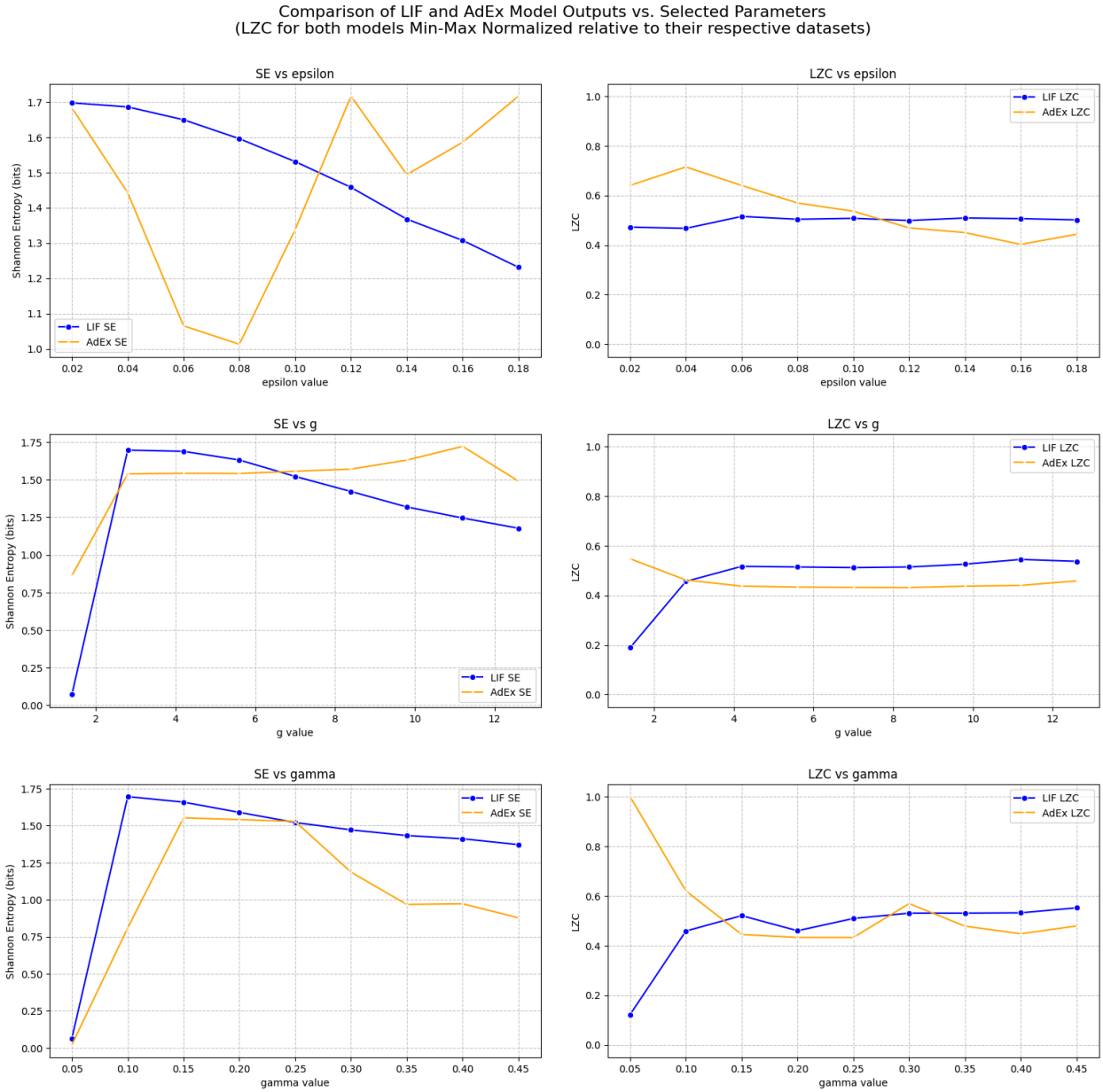

Figure 2. AdEx and LIF parameters where SE and LZC values showed sensitivity and were visually comparable.

- **Synaptic Delay (D):** The AdEx model's SE and LZC changed more with synaptic delay than the LIF model's, where these measures stayed fairly stable. This might suggest that adaptation mechanisms in AdEx interact with signal propagation delays in a more complex way to shape overall network predictability and pattern diversity.
- **Excitatory Synaptic Weight (J):** The AdEx model exhibited a strong sensitivity of both SE and LZC to J, especially a sharp decline at higher J values, which was not apparent in the LIF model where both metrics remained largely flat. The decline in AdEx might be due to strong excitation pushing neurons into a saturated or overly regular firing regime,

possibly modulated by adaptation. The LIF model, without adaptation, might maintain its activity level more consistently across changes in J until a point of over-excitation leads to silence (not seen in this data range).

- **Connection Probability (epsilon):** Both models showed decreasing SE with increasing connectivity (though AdEx had a more complex curve). The effect on LZC was less consistent between the models. Increased connectivity (higher epsilon) generally promotes synchronization, which can reduce both SE and pattern diversity. AdEx's adaptive features might counteract this synchronization effect on SE to some extent at certain epsilon values, leading to its non-monotonic SE curve.
- **Relative Inhibitory Strength (g):** Both models showed that very low 'g' suppresses activity and thus SE/LZC. As 'g' increases into a more balanced regime, SE increases in both. However, AdEx SE continued to rise over a wider range of 'g' than LIF SE, which peaked earlier. For LZC, AdEx showed a decreasing trend with 'g' (after the initial low point), while LIF LZC increased and then plateaued. This divergence suggests that AdEx's adaptation might allow the network to maintain high temporal unpredictability (SE) even with strong inhibition, while this same inhibition simplifies the diversity of population firing patterns (LZC).
- **E/I Neuron Ratio (gamma - proportion of inhibitory neurons):** Both models showed suppressed activity at very low gamma (too little inhibition). SE peaked at a relatively low gamma (0.10-0.15) and then declined in both. AdEx LZC showed a unique very high peak at the lowest gamma, not seen in LIF, perhaps due to some specific unstable, diverse firing before complete suppression. For more balanced gamma values, LIF LZC tended to be higher and more stable than AdEx LZC.
- **Refractory Period (tau_rp):** Both models were largely insensitive to variations in the refractory period in terms of SE and LZC within the tested ranges, suggesting it's not a primary driver of these complexity measures once it's within a reasonable physiological range.
- **Firing Threshold (theta in LIF / V_T in AdEx):** The LIF model showed clear sensitivity to its firing threshold 'theta', with SE and LZC increasing as the threshold made firing more difficult (up to a point). The AdEx model, over its tested V_T range, was surprisingly insensitive. This might be because the AdEx model's exponential term and adaptation current (w) create a more dynamic and "softer" effective threshold compared to the hard threshold in the LIF model.

Comparing the AdEx and LIF models reveals key differences in their responses to parameter variations, primarily due to the AdEx model's adaptive mechanisms. The AdEx model generally showed greater sensitivity and more complex, often non-monotonic, SE and LZC responses, especially to synaptic delay (D) and excitatory synaptic weight (J), where LIF model metrics

were flatter or simpler.

Although both models showed suppressed activity with low inhibitory strength (g) or E/I ratios (gamma), the AdEx model often maintained higher SE over broader ranges and exhibited unique LZC behaviors (e.g., a peak at very low gamma), suggesting its adaptation allows more varied firing regimes. Conversely, the refractory period (tau_rp) minimally impacted SE and LZC in both models. A notable divergence occurred with the firing threshold: the LIF model was sensitive to its threshold (theta), whereas the AdEx model remained largely insensitive to V_T variations, likely due to its dynamic effective threshold arising from adaptation and exponential spike initiation.

These distinctions highlight neuronal adaptation (via AdEx parameters 'a', 'b', and 'τw') as a crucial factor in shaping network informational dynamics. By introducing history-dependence and richer single-neuron firing patterns, adaptive properties interact intricately with network parameters and inputs. This explains the observed divergences in global complexity measures (SE, LZC) compared to a simpler non-adaptive model, underscoring the importance of including adaptive features when modeling neural complexity.

4. Conclusion

The results from our simulations show that changing various parameters in the AdEx model can significantly alter Spike Train Entropy (SE), and Lempel-Ziv Complexity (LZC). Notably, these two distinct measures of complexity do not always change in concert; their relationship is highly dependent on the specific neural parameter being adjusted. Having adaptive mechanisms in the AdEx model seems to lead to more complex reactions compared to simpler models without adaptation, like the LIF neuron.

Interpreting Parameter Effects on SE and LZC in AdEx and Comparison with LIF:

Our findings highlight that key network-level parameters like excitatory synaptic weight (J), relative inhibitory strength (g), the E/I neuron ratio (gamma), synaptic delay (D), and connection probability (epsilon) were the main drivers of changes in SE and LZC in the AdEx model. Often, there was a trade-off: conditions that promoted high SE (meaning more unpredictable network spike counts over time) frequently resulted in lower LZC (meaning less diversity in the moment-to-moment firing patterns of the whole neuron population). This was particularly noticeable in states with balanced excitation and inhibition (gamma around 0.15-0.25), which had high SE but relatively low LZC.

Comparing these AdEx results to those from a non-adaptive LIF model provides valuable insights. For instance, the AdEx model showed greater sensitivity in SE and LZC to synaptic delay (D) and excitatory synaptic weight (J) compared to the LIF model, where these measures

were often more stable. This suggests that AdEx's adaptive currents interact with these fundamental synaptic parameters to produce more varied outcomes in network complexity. When varying relative inhibitory strength (g) or the E/I ratio (gamma), both models showed that insufficient inhibition suppressed activity. However, the AdEx model often maintained higher SE across a broader range of inhibition, or showed unique LZC peaks (like at very low gamma), likely due to its adaptive capabilities allowing for more diverse firing regimes before full suppression or over-synchronization. In contrast, parameters like the refractory period (tau_rp) had minimal impact on SE and LZC in both models, suggesting these measures are robust to small changes in this specific neuronal property once it's within a typical range. The difference in sensitivity to the firing threshold (V_T in AdEx vs. theta in LIF) was also notable, with AdEx being less sensitive, possibly due to its "softer" effective threshold shaped by adaptation and the exponential spike initiation term.

The preliminary exploration of spike threshold (V_T), subthreshold adaptation (a), and noise intensity (sigma) involved a restricted set of three values for each. Consequently, the apparent lack of substantial effect on SE and LZC for these parameters (Figure 1) should not be overinterpreted. These parameters warrant a more thorough investigation with a broader range of values to reliably assess their contribution to network complexity measures.

The adaptive mechanisms of the AdEx model (governed by parameters like 'a', 'b', and 'τw'), which allow neurons to change their firing behavior based on past activity (Naud et al., 2008), are likely central to these observations. These mechanisms can create rich and varied temporal patterns in individual spike trains (contributing to SE), but they might also lead to more regular or constrained patterns of activity across the entire population at any given moment. This could explain why high SE sometimes appeared with lower LZC in AdEx, a behavior that might differ in non-adaptive models.

Relevance to the Entropic Brain Hypothesis (EBH):

The Entropic Brain Hypothesis (EBH) proposes that conscious states are associated with high levels of entropy in brain activity, reflecting a more flexible and rich cognitive state (Carhart-Harris, 2018). Often, empirical tests of the EBH utilize complexity measures derived from global brain signals like EEG or MEG, such as LZC applied to the continuous time series. Our study offers a different perspective by examining SE alongside an LZC measure focused on the diversity of fine-grained, instantaneous neuronal co-activation patterns. The EBH might imply that various measures of neural 'randomness' or 'complexity' would increase together in such states; however, the specific nature of the complexity measure used is crucial.

Our AdEx simulation results offer a mixed perspective when considered in light of the EBH:

- **Partial support under specific conditions:**
    - The strong positive correlation between SE and LZC when varying the excitatory synaptic weight (J) in the AdEx model could be seen as consistent with the EBH, suggesting that, for this parameter, changes leading to more unpredictable activity also lead to more diverse firing patterns.
    - We also identified specific AdEx parameter settings, like very sparse connectivity (low epsilon), that could produce simultaneously high SE and high LZC while maintaining plausible firing rates. These particular states might align with the EBH's prediction of enriched and complex neural dynamics.
- **Observations posing nuances for a simple EBH interpretation:**
    - The frequent negative correlations between SE and LZC (reflecting diversity of population firing patterns) for several key parameters in the AdEx model (D, g, gamma) suggest that not all aspects of 'entropy' or 'complexity' necessarily increase together. For example, increasing overall inhibition often increased SE but decreased the repertoire of distinct population firing patterns (LZC). This implies that a network can become more unpredictable in its overall activity over time (higher SE) while simultaneously utilizing a less diverse set of instantaneous population states (lower LZC).
    - In AdEx states with balanced excitation and inhibition (gamma = 0.15-0.25), often considered to reflect a typical cortical operating regime, we observed high SE but low LZC (low diversity of firing patterns). If high values of multiple, distinct types of complexity measures are markers of the 'entropic brain' states, then these balanced states in our model, despite their high temporal unpredictability (SE), present a more complex picture due to their relatively restricted repertoire of population codes (LZC).

The comparison with the LIF model further adds to this nuanced view. The LIF model, lacking adaptation, often showed simpler or flatter responses. If EBH implies a general increase in various complexity facets, the more complex and sometimes decoupled SE/LZC relationships in AdEx highlight that specific neuronal mechanisms (like adaptation) can significantly shape how "entropy" manifests. This challenges a monolithic interpretation of 'brain entropy.' It suggests that 'entropy' or 'complexity' in the context of brain states is multifaceted, and the route to, and nature of, high-entropy states might be mechanistically diverse, depending on whether one considers temporal unpredictability of global signals or the diversity of underlying neuronal population codes. The varied results from human neuroimaging studies on the EBH (McCulloch et al., 2023) also show how complex these connections are in actual biological systems. The adaptive mechanisms in the AdEx model (Ladenbauer et al., 2014) likely contribute significantly to the observed decoupling between SE and LZC.

Critical Perspective on Biological Relevance:

It is important to reiterate the need for caution when relating these findings directly to the biological brain. The AdEx model, while incorporating adaptation—a key biological feature—is still a simplified representation of real neurons. The specific configuration of our model was primarily guided by the aim of ensuring comparability with an earlier LIF project (Wierzchula et al., 2024). This means that the parameter values and network setup are not intended to perfectly replicate any particular biological brain region or state. (While some output characteristics like MFR from our baseline AdEx model might fall within broad ranges reported for cortical activity (e.g., Buzsáki & Mizuseki, 2014; Zerlaut et al., 2018), this was not the primary goal of the parameterization).

Therefore, observations from our model—such as high SE and low LZC in "balanced E/I states"—are characteristics of *this particular computational model* under its specific setup. These findings can generate hypotheses or offer analogies for how real neural systems *might* behave, but they are not direct measurements of biological activity. The advantage of this modeling method is that it lets us systematically explore how changing specific parameters affects complex results (SE and LZC) in a controlled computer simulation. This helps in building theoretical understanding and can guide future experimental design, but direct biological claims should be made with considerable care.

The LZC metric used here reflects the diversity of *instantaneous population codes* (patterns of firing across neurons at one moment). The SE metric reflects the unpredictability of *network-wide spike counts over longer time bins*. The fact that these can be decoupled in our AdEx simulations underscores that "neural complexity" or "signal diversity" is not a single, uniform property but has multiple facets.

Limitations of the Study

This study, like all computational modeling work, has several limitations that should be considered when interpreting the results:

- **Model Simplification:** The AdEx model, despite its inclusion of adaptation, does not capture the full complexity of biological neurons. Factors like detailed dendritic structures and computations, the variety of ion channels, multiple adaptation timescales, and metabolic constraints are not explicitly included (Brette & Gerstner, 2005; Naud et al., 2008).
- **LFP Approximation:** The method used to calculate the Local Field Potential is an approximation based on summing kernel-convolved spike trains (Telenczuk et al., 2020). It does not model the detailed biophysics of LFP generation, which involves complex

current flows and volume conduction in brain tissue.

- **Parameter Ranges and Baseline Choice:** We explored specific ranges for each parameter around a baseline chosen for comparability with a previous LIF study (Wierzchula et al., 2024). The network's behavior and sensitivity to parameters might differ outside these explored ranges or with a different baseline configuration.
- **LZC Definition and Calculation:** The LZC metric in this study was specifically defined to quantify the diversity of instantaneous population firing patterns (sequences of binary vectors representing active neurons at each 0.1 ms time step). This approach differs from other methods of calculating LZC, such as those applied to a single, continuous LFP time series in some experimental studies (e.g., Schartner et al., 2017). These different LZC methodologies, or other complexity measures entirely, might capture distinct aspects of network dynamics.
- **Limited Scope of Intrinsic Parameter Effects:** For some intrinsic AdEx parameters (V_T, 'a', sigma, tau_rp), we observed minimal impact on the global SE and LZC measures. This could be due to the network operating in a state where it was not highly sensitive to these particular parameters, the chosen output measures not being the most appropriate for revealing their effects, or the parameter ranges tested not being wide enough to elicit significant changes in these global metrics.
- **Absence of Structural Plasticity:** The study used static network connectivity. In biological systems, synaptic strengths and even connections can change over time (plasticity), which would further influence network dynamics and information processing.
- **Computational Constraints:** Simulating larger, more detailed networks or exploring a vastly larger parameter space was limited by computational resources.

Future Work

The findings and limitations of this study open up several avenues for future research:

- **Broader Parameter Exploration:** Investigate a wider range of values for the parameters studied, and explore the effects of varying combinations of parameters simultaneously, which might reveal more complex interactions.
- **Different Complexity Measures:** Implement and compare results using other measures of entropy (e.g., LZC applied directly to the LFP time series, permutation entropy of spike trains) and signal diversity to gain a more comprehensive understanding of the network's informational dynamics.
- **Explicit LIF vs. AdEx Comparison:** Conduct a more detailed and direct comparative study by simulating both LIF and AdEx models under an identical and extensive set of parameter variations and input conditions, specifically designed to isolate the effects of adaptation.

- **Task-Based Performance:** Investigate how the observed changes in SE and LZC correlate with the network's ability to perform specific computational tasks, such as pattern recognition, signal discrimination, or information transmission.
- **More Complex Network Architectures:** Explore networks with more biologically inspired architectures, such as layered structures or specific connectivity motifs, rather than purely random connectivity.
- **Inclusion of Plasticity:** Incorporate synaptic plasticity rules (e.g., spike-timing-dependent plasticity) into the AdEx network to study how learning and adaptation of synaptic weights interact with intrinsic neuronal adaptation to shape entropy and complexity over time.

In conclusion, this thesis carefully studied how important neuron and network settings affect different aspects of complexity in AdEx neural network models. We looked at how unpredictable the timing of overall activity is (Shannon Entropy or SE) and how varied the neuron firing patterns are (Lempel-Ziv Complexity or LZC). Our results show that these two ways of measuring complexity don't always act as one; they often change differently when we adjust parameters. The ability of neurons to adapt their responses, which is a feature of the AdEx model, plays a big part in these varied reactions, especially when compared to simpler LIF models. Although using a simplified model and specific ways to measure complexity has its limits, this study highlights how important it is to use exact and varied methods to measure complexity in computational neuroscience. In the end, this research helps us better understand how specific details of neurons and networks create the complex and varied activity needed for brain-like systems to process information. It also offers a clearer way to look at ideas like the Entropic Brain Hypothesis.

References

Aamodt, A., Nilsen, A. S., Thürer, B., Moghadam, F. H., Kauppi, N., Juel, B. E., & Storm, J. F. (2021). EEG signal diversity varies with sleep stage and aspects of dream experience. *Frontiers in Psychology, 12*, 655884. https://doi.org/10.3389/fpsyg.2021.655884

Brette, R., & Gerstner, W. (2005). Adaptive exponential integrate-and-fire model as an effective description of neuronal activity. *Journal of Neurophysiology*, *94*(5), 3637–3642. https://doi.org/10.1152/jn.00686.2005

Brunel, N. (2000). Dynamics of sparsely connected networks of excitatory and inhibitory spiking neurons. *Journal of Computational Neuroscience, 8*(3), 183–208. https://doi.org/10.1023/A:1008925309027

Buzsáki, G., & Mizuseki, K. (2014). The log-dynamic brain: How skewed distributions affect network operations. *Nature Reviews Neuroscience, 15*(4), 264–278. https://doi.org/10.1038/nrn3687

Carhart-Harris, R. L. (2018). The entropic brain - revisited. *Neuropharmacology, 142*, 167–178. https://doi.org/10.1016/j.neuropharm.2018.03.010

Carhart-Harris, R. L., Leech, R., Hellyer, P. J., Shanahan, M., Feilding, A., Tagliazucchi, E., Chialvo, D. R., & Nutt, D. (2014). The entropic brain: A theory of conscious states informed by neuroimaging research with psychedelic drugs. *Frontiers in Human Neuroscience, 8*, 20. https://doi.org/10.3389/fnhum.2014.00020

Fagerholm, E. D., Dezhina, Z., Moran, R. J., Turkheimer, F. E., & Leech, R. (2023). A primer on entropy in neuroscience. *Neuroscience & Biobehavioral Reviews, 146,* 105070. https://doi.org/10.1016/j.neubiorev.2023.105070

Farnes, N., Juel, B. E., Nilsen, A. S., Romundstad, L. G., & Storm, J. F. (2020). Increased signal diversity/complexity of spontaneous EEG, but not evoked EEG responses, in ketamine-induced psychedelic state in humans. *PLOS ONE, 15*(11), e0242056. https://doi.org/10.1371/journal.pone.0242056

Gerstner, W., Kistler, W. M., Naud, R., & Paninski, L. (2014). Neuronal dynamics: From single neurons to networks and models of cognition. *Cambridge University Press*. https://doi.org/10.1017/CBO9781107447615

Kalev, K., Bachmann, M., Orgo, L., Lass, J., & Hinrikus, H. (2015). Lempel-Ziv and multiscale Lempel-Ziv complexity in depression. *2015 37th Annual International Conference of the IEEE Engineering in Medicine and Biology Society (EMBC)*, 4158–4161. https://doi.org/10.1109/EMBC.2015.7319310

Ladenbauer, J., Augustin, M., & Obermayer, K. (2014). How adaptation currents change threshold, gain, and variability of neuronal spiking. *Journal of Neurophysiology, 111*(6), 1356–1371. https://doi.org/10.1152/jn.00586.2013

Lempel, A., & Ziv, J. (1976). On the complexity of finite sequences. *IEEE Transactions on Information Theory*, *22*(1), 75–81. https://doi.org/10.1109/TIT.1976.1055501

Mazzoni, A., Panzeri, S., Logothetis, N. K., & Brunel, N. (2008). Encoding of naturalistic stimuli by local field potential spectra in networks of excitatory and inhibitory neurons. *PLoS Computational Biology*, *4*(12), e1000239. https://doi.org/10.1371/journal.pcbi.1000239

McCulloch, D. E. W., Olsen, A. S., Ozenne, B., Stenbæk, D. S., Armand, S., Madsen, M. K., ... & Fisher, P. M. (2023). Navigating the chaos of psychedelic neuroimaging: A multi-metric evaluation of acute psilocybin effects on brain entropy. *MedRxiv*, 2023-07. https://doi.org/10.1101/2023.07.03.23292164 [Preprint]

Naud, R., Marcille, N., Clopath, C., & Gerstner, W. (2008). Firing patterns in the adaptive exponential integrate-and-fire model. *Biological Cybernetics, 99*(4–5), 335–347. https://doi.org/10.1007/s00422-008-0264-7

Ruffini, G., Damiani, G., Lozano-Soldevilla, D., Deco, N., Rosas, F. E., Kiani, N. A., Ripollés, P., Insabato, A., Noy, N., Nuiten, S., Tagliazucchi, E., & Deco, G. (2023). LSD-induced increase of Ising temperature and algorithmic complexity of brain dynamics. *PLoS Computational Biology, 19*(2), e1010811. https://doi.org/10.1371/journal.pcbi.1010811

Sabeti, M., Katebi, S., & Boostani, R. (2009). Entropy and complexity measures for EEG signal classification of schizophrenic and control participants. *Artificial Intelligence in Medicine, 47*(3), 263–274. https://doi.org/10.1016/j.artmed.2009.03.003

Singleton, S. P., Luppi, A. I., Carhart-Harris, R. L., Cruzat, J., Roseman, L., Nutt, D. J., Deco, G., Kringelbach, M. L., Stamatakis, E. A., & Kuceyeski, A. (2022). Receptor-informed network control theory links LSD and psilocybin to a flattening of the brain's control energy landscape. *Nature Communications*, *13*, 5812. https://doi.org/10.1038/s41467-022-33578-1

Schartner, M. M., Carhart-Harris, R. L., Barrett, A. B., Seth, A. K., & Muthukumaraswamy, S. D. (2017). Increased spontaneous MEG signal diversity for psychoactive doses of ketamine, LSD and psilocybin. *Scientific Reports, 7*(1), 46421. https://doi.org/10.1038/srep46421

Stimberg, M., Brette, R., & Goodman, D. F. M. (2019). Brian 2, an intuitive and efficient neural simulator. *eLife*, *8*, e47314. https://doi.org/10.7554/eLife.47314

Telenczuk, B., Telenczuk, M., & Destexhe, A. (2020). A kernel-based method to calculate local field potentials from networks of spiking neurons. *Journal of Neuroscience Methods,* 344, 108871. https://doi.org/10.1016/j.jneumeth.2020.108871

Tononi, G., Sporns, O., & Edelman, G. M. (1994). A measure for brain complexity: relating functional segregation and integration in the nervous system. *Proceedings of the National Academy of Sciences, 91*(11), 5033–5037. https://doi.org/10.1073/pnas.91.11.5033

Touboul, J., & Brette, R. (2008). Dynamics and bifurcations of the adaptive exponential integrate-and-fire model. *Biological Cybernetics, 99*(4-5), 319–334. https://doi.org/10.1007/s00422-008-0267-4

Vogels, T. P., & Abbott, L. F. (2005). Signal propagation and logic gating in networks of

integrate-and-fire neurons. *Journal of Neuroscience*, *25*(46), 10786–10795. https://doi.org/10.1523/JNEUROSCI.3508-05.2005

Zerlaut, Y., Chemla, S., Chavane, F., & Destexhe, A. (2018). Modeling mesoscopic cortical dynamics using a mean-field model of conductance-based networks of adaptive exponential integrate-and-fire neurons. *Journal of Computational Neuroscience, 44*(1), 45–61. https://doi.org/10.1007/s10827-017-0668-2

Zhang, X. S., Roy, R. J., & Jensen, E. W. (2001). EEG complexity as a measure of depth of anesthesia. *IEEE Transactions on Biomedical Engineering*, *48*(12), 1424–1433. https://doi.org/10.1109/10.966601

Wierzchula, A., Kaljo, M., Siemund, B., Van Iseghem, E., & Junk, H. (2024). *Entropy and signal diversity in the biological brain* [Unpublished project paper for Natural and Artificial Intelligence, Project Nr. 25]. *University of Tartu*. Available: https://docs.google.com/document/d/1w69KkEhsJClMiqvPdwwHno20LEqOoco7CfFUsSj3uEI/edit?usp=sharing

Appendices

Appendix 1: adex_simulation_py (main script for AdEx configuration)

```
#!/gpfs/helios/home/aresh/magister_env/bin/python
from brian2 import second, mV, Hz, pF, nS, pA, nA, ms, mvolt, hertz, farad,
siemens, NeuronGroup, Synapses, SpikeMonitor, PopulationRateMonitor, run,
PoissonInput
# from brian2 import * - gives errors for some reason so all separate what
needed
import numpy as np
from scipy.stats import entropy
from scipy.signal import hilbert
import pandas as pd
import h5py
import argparse
import logging

# Setup logging for error checking
logging.basicConfig(filename='/gpfs/helios/home/aresh/magister/outputs/simulati
on.log', level=logging.ERROR)

def f_temporal_kernel(t, tau):
    return np.exp(-(t ** 2) / tau)

def calc_lfp(cells, X, Y, xe, ye, gamma=0.2, va=200, lambda_=0.2, dur=1000,
dt=0.1, amp_e=0.48, amp_i=3, sig_i=2.1, sig_e=3.15):
    npts = int(dur / dt)
    lfp_time = np.arange(npts) * dt
    dist = np.sqrt((X - xe) ** 2 + (Y - ye) ** 2)
    delay = 10.4 + dist / va
    amp = np.exp(-dist / lambda_)
    N = len(X)
    N_E = int(N * (1 - gamma))
    amp[:N_E] *= amp_i
    amp[N_E:] *= amp_e
    spt = cells['time']
    cid = cells['cellid']
    if len(spt) == 0:
        return np.zeros(npts), lfp_time
```

```
    kernel_contribs = amp[None, cid] * f_temporal_kernel(lfp_time[:, None] -
delay[None, cid] - spt[None, :], sig_i)
    lfp = kernel_contribs.sum(1)
    if np.any(np.isnan(lfp)):
        logging.error(f"LFP contains NaN for param={param}, value={value},
trial={trial}")
    return lfp, lfp_time

def compute_se(spike_times, bin_size=0.2, sim_time=1):
    if len(spike_times) == 0:
        return 0.0
    bins = np.arange(0, sim_time, bin_size)
    hist, _ = np.histogram(spike_times, bins)
    return entropy(hist + 1e-10, base=2)

def lempel_ziv_complexity(time_series):
    if isinstance(time_series, list):
        time_series = np.array(time_series)
    if np.std(time_series) == 0:
        return 0, 0
    analytic_signal = hilbert(time_series)
    amplitude_envelope = np.abs(analytic_signal)
    binary_seq = (amplitude_envelope > np.percentile(amplitude_envelope,
50.0)).astype(int)
    n = len(binary_seq)
    C = 1
    i = 0
    u = 1
    v = 1
    vmax = v
    while u + v <= n:
        if binary_seq[i + v-1] == binary_seq[u + v-1]:
            v += 1
        else:
            vmax = max(v, vmax)
            i = i + 1
            if i == u:
                C = C + 1
                u = u + vmax
                v = 1
                i = 0
```

```
                vmax = v
            else:
                v = 1
    if v != 1:
        C = C + 1
    return C / np.log2(n), C

def compute_spatial_lzc(spikes, t_steps, dt=0.1):
    lzc_vals = []
    for t in range(t_steps):
        pattern = (spikes[:, t] > 0).astype(int)
        lzc_norm, lzc_unnorm = lempel_ziv_complexity(pattern)
        lzc_vals.append(lzc_norm)
    return np.mean(lzc_vals), np.mean([v * np.log2(len(pattern)) for v in
lzc_vals])

def compute_multi_lzc(spikes, n_groups=10):
    group_size = spikes.shape[0] // n_groups
    lzc_vals = []
    for t in range(spikes.shape[1]):
        pattern = []
        for g in range(n_groups):
            group = spikes[g*group_size:(g+1)*group_size, t]
            pattern.extend(group > 0)
        lzc_norm, lzc_unnorm = lempel_ziv_complexity(np.array(pattern))
        lzc_vals.append(lzc_norm)
    return np.mean(lzc_vals), np.mean([v * np.log2(len(pattern)) for v in
lzc_vals])

def setup_adex_model(N=1000, epsilon=0.1, gamma=0.2, g=5, J=0.04*mV, D=1.5*ms,
tau_m=20*ms, tau_rp=2*ms, neuron_type='mixed', sigma=0.1*nA, **kwargs):
    N_E = int(N * (1 - gamma))
    N_I = N - N_E
    C = np.zeros(N) * pF
    g_L = np.zeros(N) * nS
    E_L = np.zeros(N) * mV
    V_T = np.zeros(N) * mV
    Delta_T = np.zeros(N) * mV
    a = np.zeros(N) * nS
    tau_w = np.zeros(N) * ms
    b = np.zeros(N) * nA
```

```
    V_r = np.zeros(N) * mV
    tau_rp = np.zeros(N) * ms

    if neuron_type == 'mixed':
        C[:N_E] = 150*pF
        g_L[:N_E] = 10*nS
        E_L[:N_E] = -65*mV
        V_T[:N_E] = -50*mV
        Delta_T[:N_E] = 2*mV
        a[:N_E] = 2*nS
        tau_w[:N_E] = 500*ms
        b[:N_E] = 0.01*nA
        V_r[:N_E] = -60*mV
        tau_rp[:N_E] = 2*ms
        C[N_E:] = 100*pF
        g_L[N_E:] = 10*nS
        E_L[N_E:] = -65*mV
        V_T[N_E:] = -42*mV
        Delta_T[N_E:] = 2*mV
        a[N_E:] = 0*nS
        tau_w[N_E:] = 15*ms
        b[N_E:] = 0*nA
        V_r[N_E:] = -65*mV
        tau_rp[N_E:] = 1*ms
    else: #Can configure 4 different types of neurons when needed
        if neuron_type == 'RS':
            C[:] = 150*pF
            g_L[:] = 10*nS
            E_L[:] = -65*mV
            V_T[:] = -50*mV
            Delta_T[:] = 2*mV
            a[:] = 2*nS
            tau_w[:] = 500*ms
            b[:] = 0.01*nA
            V_r[:] = -60*mV
            tau_rp[:] = 2*ms
        elif neuron_type == 'IB':
            C[:] = 200*pF
            g_L[:] = 10*nS
            E_L[:] = -60*mV
            V_T[:] = -50*mV
```

```
            Delta_T[:] = 2*mV
            a[:] = 2*nS
            tau_w[:] = 120*ms
            b[:] = 0.1*nA
            V_r[:] = -50*mV
            tau_rp[:] = 2*ms
        elif neuron_type == 'TC':
            C[:] = 200*pF
            g_L[:] = 10*nS
            E_L[:] = -65*mV
            V_T[:] = -55*mV
            Delta_T[:] = 2*mV
            a[:] = 2*nS
            tau_w[:] = 120*ms
            b[:] = 0.01*nA
            V_r[:] = -65*mV
            tau_rp[:] = 2*ms
        elif neuron_type == 'FS':
            C[:] = 100*pF
            g_L[:] = 10*nS
            E_L[:] = -65*mV
            V_T[:] = -42*mV
            Delta_T[:] = 2*mV
            a[:] = 0*nS
            tau_w[:] = 15*ms
            b[:] = 0*nA
            V_r[:] = -65*mV
            tau_rp[:] = 1*ms

    C_E = epsilon * N_E
    C_ext = C_E
    V_T_RS = -50 * mV
    E_L_RS = -65 * mV
    nu_thr = (V_T_RS - E_L_RS) / (J * C_E * tau_m)
    nu_ext = 1.5 * np.clip(nu_thr / hertz, 0, 1000) * hertz

    eqs = '''
    dvm/dt = (g_L * (E_L - vm) + g_L * Delta_T * exp((vm - V_T)/Delta_T) - w) /
C : volt (unless refractory)
    dw/dt = (a * (vm - E_L) - w) / tau_w : amp
    Vcut = V_T + 5 * Delta_T : volt
```

```
    C : farad
    g_L : siemens
    E_L : volt
    V_T : volt
    Delta_T : volt
    a : siemens
    tau_w : second
    b : amp
    V_r : volt
    tau_rp : second
    '''

    G = NeuronGroup(N, eqs, threshold='vm > Vcut', reset='vm = V_r; w += b',
refractory='tau_rp', method='euler')
    G.vm = E_L
    G.w = 0*pA
    G.C = C
    G.g_L = g_L
    G.E_L = E_L
    G.V_T = V_T
    G.Delta_T = Delta_T
    G.a = a
    G.tau_w = tau_w
    G.b = b
    G.V_r = V_r
    G.tau_rp = tau_rp

    S_exc = Synapses(G[:N_E], G, on_pre='vm += J', delay=D, namespace={'J': J})
    S_inh = Synapses(G[N_E:], G, on_pre='vm += -g*J', delay=D, namespace={'J':
J, 'g': g})
    S_exc.connect(p=epsilon)
    S_inh.connect(p=epsilon)

    P = PoissonInput(target=G, target_var='vm', N=C_ext, rate=nu_ext, weight=J)

    return G, S_exc, S_inh, P

def main():
    parser = argparse.ArgumentParser(description='AdEx Simulation')
    parser.add_argument('--N', type=int, default=5000, help='Number of
neurons')
```

```
    parser.add_argument('--param', type=str, default='baseline',
help='Parameter to vary')
    parser.add_argument('--value', type=float, default=0, help='Parameter
value')
    parser.add_argument('--trial', type=int, default=1, help='Trial number')
    parser.add_argument('--J', type=float, default=0.04, help='Synaptic weight
(mV)')
    args = parser.parse_args()

    global param, value, trial
    N = args.N
    param = args.param
    value = args.value
    trial = args.trial
    J = args.J * mV

    sim_time = 1*second
    output_prefix = f"isolated/{param}_{value}_trial{trial}"

    kwargs = {'N': N, 'neuron_type': 'mixed', 'J': J}
    if param != 'baseline':
        if param in ['V_T', 'J']:
            kwargs[param] = value * mV
        elif param in ['D', 'tau_m', 'tau_rp']:
            kwargs[param] = value * ms
        else:
            kwargs[param] = value

    gamma = kwargs.get('gamma', 0.2)
    N_E = int(N * (1 - gamma))
    N_I = N - N_E
    try:
        G, S_exc, S_inh, P = setup_adex_model(**kwargs)
    except TypeError as e:
        logging.error(f"TypeError in setup_adex_model for param={param},
value={value}, trial={trial}: {e}")
        raise

    M = SpikeMonitor(G)
    R = PopulationRateMonitor(G)
    run(sim_time, report='text')
```

```
    # Clip vm and w to prevent NaN using unit-aware assignment
    G.vm = np.clip(G.vm/mV, -100, 100) * mV
    G.w = np.clip(G.w/nA, -10, 10) * nA

    if np.any(np.isnan(G.vm)) or np.any(np.isnan(G.w)):
        logging.error(f"NaN detected in vm or w for param={param},
value={value}, trial={trial}")

    firing_rate = len(M.t) / (N * sim_time / second)

    X, Y = np.random.rand(2, N) * 0.2
    xe, ye = 0.1, 0.1
    cells = np.zeros(len(M.t), dtype=[('cellid', 'i4'), ('time', 'f8')])
    cells['cellid'] = M.i[:]
    cells['time'] = M.t[:] / second
    lfp, lfp_time = calc_lfp(cells, X, Y, xe, ye, gamma=gamma)

    lfp_mean = np.mean(lfp)
    lfp_std = np.std(lfp)

    se = compute_se(M.t / second, bin_size=0.2, sim_time=sim_time / second)
    lzc_normalized, lzc_unnormalized = lempel_ziv_complexity(lfp)

    spike_matrix = np.zeros((N, int(sim_time / (0.1*ms))))
    for i, t in zip(M.i, M.t):
        t_idx = int(t / (0.1*ms))
        if t_idx < spike_matrix.shape[1]:
            spike_matrix[i, t_idx] = 1
    lzc_spatial_normalized, lzc_spatial_unnormalized =
compute_spatial_lzc(spike_matrix, spike_matrix.shape[1])
    lzc_multi_normalized, lzc_multi_unnormalized =
compute_multi_lzc(spike_matrix, n_groups=10)

    output = pd.DataFrame([{
        'param': param,
        'value': value,
        'entropy': se,
        'lzc_temporal_normalized': lzc_normalized,
        'lzc_temporal_unnormalized': lzc_unnormalized,
        'lzc_spatial_normalized': lzc_spatial_normalized,
```

```
        'lzc_spatial_unnormalized': lzc_spatial_unnormalized,
        'lzc_multi_normalized': lzc_multi_normalized,
        'lzc_multi_unnormalized': lzc_multi_unnormalized,
        'firing_rate': firing_rate,
        'lfp_mean_uv': lfp_mean,
        'lfp_std_uv': lfp_std
    }])

output.to_csv(f"/gpfs/helios/home/aresh/magister/outputs/{output_prefix}_metrics.csv", index=False)
    with h5py.File(f"/gpfs/helios/home/aresh/magister/outputs/{output_prefix}_lfp.h5", 'w') as f:
        f.create_dataset('lfp', data=lfp)
        f.create_dataset('lfp_time', data=lfp_time)

    print(f"Param: {param}, Value: {value}, Trial: {trial}, "
          f"Firing Rate: {firing_rate:.2f} Hz, SE: {se:.2f} bits, "
          f"Temporal LZC: {lzc_normalized:.3f}, Unnormalized: {lzc_unnormalized}, "
          f"Spatial LZC: {lzc_spatial_normalized:.3f}, Unnormalized: {lzc_spatial_unnormalized:.1f}, "
          f"Multi LZC: {lzc_multi_normalized:.3f}, Unnormalized: {lzc_multi_unnormalized:.1f}, "
          f"LFP Mean: {lfp_mean:.2f} µV, Std: {lfp_std:.2f} µV")

if __name__ == '__main__':
    main()
```

Appendix 2: submit_experiments.sh (Simulation parameter definitions and cycle logic)

```
#!/bin/bash
# Parameter ranges aligned with output_5000.txt and AdEx neuron types (Naud et
al., 2008; Gerstner et al., 2014)
params=("epsilon:0.02,0.04,0.06,0.08,0.1,0.12,0.14,0.16,0.18"  # Connection
probability, from original study
        "gamma:0.05,0.1,0.15,0.2,0.25,0.3,0.35,0.4,0.45"  # Inhibitory
fraction, balances network
        "g:1.4,2.8,4.2,5.6,7,8.4,9.8,11.2,12.6"  # Inhibitory strength,
modulates inhibition
        "J:0.02,0.04,0.06,0.08,0.1,0.12,0.14,0.16,0.18"  # Synaptic weight,
scales inputs
        "D:0.3,0.6,0.9,1.2,1.5,1.8,2.1,2.4"  # Transmission delay, models
propagation
        "tau_rp:0.4,0.8,1.2,1.6,2,2.4,2.8,3.2,3.6"  # Refractory period, limits
firing
        "V_T:-55,-50,-45"  # Spike threshold, spans RS/TC (-55 to -50 mV) and
FS (-45 mV)
        "a:0,2,4"  # Subthreshold adaptation, 0 for FS, 2-4 nS for RS/IB/TC
        "b:0,0.1,0.2"  # Spike-triggered adaptation, 0 for FS, 0.01-0.1 nA for
RS/IB/TC
        "sigma:0,0.1,0.2")  # Noise intensity, adds stochasticity
for param_entry in "${params[@]}"; do
    param=${param_entry%%:*}
    values=${param_entry#*:}
    IFS=',' read -r -a value_array <<< "$values"
    for value in "${value_array[@]}"; do
        for trial in {1..3}; do
            sed -i
"s/--job-name=\\\"adex_.*\\\"/--job-name=\\\"adex_${param}_${value}_${trial}\\\
"/" run_adex.sh
            sed -i "s/python src\\/adex_simulation.py .*/python
src\\/adex_simulation.py --N 5000 --param ${param} --value ${value} --trial
${trial}/" run_adex.sh
            sbatch run_adex.sh
        done
    done
done
```

Appendix 3: run_adex.sh (HPC simulation settings)

```
#!/bin/bash -l
#SBATCH --job-name="adex_trial_%a"
#SBATCH --time=03:00:00
#SBATCH --partition=gpu
#SBATCH --gres=gpu:tesla:1
#SBATCH --cpus-per-task=4
#SBATCH --mem-per-cpu=16GB
#SBATCH --output=/gpfs/helios/home/aresh/magister/outputs/slurm-%j.out
#SBATCH --error=/gpfs/helios/home/aresh/magister/outputs/slurm-%j.err
#SBATCH --array=1-3

module purge
module load python/3.9.9
cd /gpfs/helios/home/aresh/magister
source magister_env/bin/activate
mkdir -p /gpfs/helios/home/aresh/magister/outputs/isolated
srun python src/adex_simulation.py --N 5000 --param baseline --value 0 --trial
$SLURM_ARRAY_TASK_ID
```

Appendix 4: HPC setup (pre simulations environment setup for HPC machine)

```
# HPC setup (run step by step on cluster terminal)
# Connect to Rocket cluster
ssh $username@rocket.hpc.ut.ee

# Create project directory
mkdir -p /gpfs/helios/home/$username/magister
cd /gpfs/helios/home/$username/magister

# Copy files to HPC (from local machine), use WinSCP or rsync

# Load correct working Python and check version
module load python/3.9.9
python --version

# Create virtual environment
python -m venv magister_env

# Delete virtual environment (if needed):
rm -rf magister_env

# Activate virtual environment
source magister_env/bin/activate

# Create project structure
mkdir src data outputs

# Install dependencies
pip install --upgrade pip
pip install numpy==1.23.5 brian2==2.6.0 scipy pandas h5py #Otherwise errors
pip list #Check that all dependencies are correct

# Deactivate virtual environment
deactivate

# Submit the job
sbatch run_adex.sh

# Monitor job status
squeue --me
```

Appendix 5: LIF output

LINK to output file:
https://drive.google.com/file/d/1VY89oOuNOGatUcEvFVNFc0x7hhcjPzzn/view?usp=sharing

Licence

Lihtlitsents lõputöö reprodutseerimiseks ja üldsusele kättesaadavaks tegemiseks

Mina, Ares Hubel ,
(autori nimi)

1. annan Tartu Ülikoolile tasuta loa (lihtlitsentsi) minu loodud teose

   Exploring Entropy and Signal Diversity in Neural Networks Using the AdEx Model ,
   (lõputöö pealkiri)

   mille juhendaja(d) on Karl Kristjan Kaup ,
   (juhendaja nimi)

   reprodutseerimiseks eesmärgiga seda säilitada, sealhulgas lisada Tartu Ülikooli digitaalarhiivi kuni autoriõiguse kehtivuse lõppemiseni;

2. annan Tartu Ülikoolile loa teha punktis 1 nimetatud teos üldsusele kättesaadavaks Tartu Ülikooli veebikeskkonna, sealhulgas digitaalarhiivi kaudu Creative Commonsi litsentsiga CC BY NC ND 4.0, mis lubab autorile viidates teost reprodutseerida, levitada ja üldsusele suunata ning keelab luua tuletatud teost ja kasutada teost ärieesmärgil, kuni autoriõiguse kehtivuse lõppemiseni;

3. olen teadlik, et punktides 1 ja 2 nimetatud õigused jäävad alles ka autorile;

4. kinnitan, et lihtlitsentsi andmisega ei riku ma teiste isikute intellektuaalomandi ega isikuandmete kaitse õigusaktidest tulenevaid õigusi.

Ares Hubel
15.05.2025